Transport and Communications Science Journal, Vol.77, Issue 01 (01/2026), 43-57

Transport and Communications Science Journal

EVALUATION OF DOWEL BAR DIAMETER AND SPACING EFFECTS ON THE STRESS AND DEFLECTION OF AIRFIELD RIGID PAVEMENTS USING THE FINITE ELEMENT METHOD

Tien Dung Vo[1], V. V. Tatarinov[1], Van Hieu Nguyen[2*], Van Thuy Do[2], Hong Minh Nguyen[3]

[1]Moscow Automobile and Road Construction State Technical University, No 64 Leningradsky Avenue, Moscow, Russia

[2]Le Quy Don Technical University, No 236 Hoang Quoc Viet Street, Hanoi, Vietnam

[3]Vietnam Association on Aviation Science and Technology - VAAST, No 121 Nguyen Son Street, Hanoi, Vietnam

ARTICLE INFO

TYPE: Research Article
Received: 20/10/2025
Revised: 25/11/2025
Accepted: 12/01/2026
Published online: 15/01/2026
https://doi.org/10.47869/tcsj.77.1.4
* *Corresponding author*
Email: hieunv@lqdtu.edu.vn; Tel: +84 989855883

Abstract. Mitigating the effects of thermal stress and shrinkage in airfield concrete pavements typically involves dividing the pavement into individual slabs of appropriate dimensions. Under aircraft wheel loading, the slab edges and corners are subjected to the most critical and unfavorable stress states. To reduce these disadvantages, dowel bars must be placed along both the longitudinal and transverse joints to transfer part of the applied load from the loaded slab to the adjacent one. Improper selection of dowel diameter or spacing can significantly diminish the pavement's load-bearing capacity and shorten its service life. In this study, the finite element software ABAQUS was used to examine the influence of dowel bar diameter and spacing on the stress and deflection responses of airfield concrete slabs subjected to B737-500 aircraft loading. The numerical model considered two commonly used slab thicknesses: 0.30 m and 0.40 m. The results indicate that, for a constant dowel diameter, the deflection and stress increase sharply as dowel spacing increases from 0.1 m to 0.4 m, while changes become negligible beyond 0.40 m. Conversely, when spacing is kept constant, increasing the dowel diameter from 20 mm to 40 mm substantially reduces stress and deflection, with further increases yielding minimal additional benefit. These findings provide useful guidance for selecting appropriate dowel dimensions in the design of airfield concrete pavements.

Keywords: Airfield rigid pavement, dowel bars, finite element method, stress, deflection.

1. INTRODUCTION

In airfield concrete pavement structures, joints reinforced with dowel bars constitute critical elements that govern load transfer efficiency between slabs, thereby influencing the local stress-strain response at slab edges. Unlike conventional highway pavements, airfield pavement systems operate under particularly harsh conditions, characterized by high intensity loads, frequent repetition cycles, and the need for long-term operational stability. Modern airports must accommodate wide-body aircraft, which impose large wheel loads, high operating frequency, and surface flatness requirements that are much more stringent than those of highways. Therefore, finding the structurally optimal diameter and spacing of dowel bars becomes a key technical issue in the design and rehabilitation of airport rigid pavements.

If the dowel bars across the joints are ineffective, the loads are not properly transferred between slabs, leading to increased local bending and shear stresses, reduced structural service life, and cracking at slab edges. When an aircraft wheel acts near a joint, a slab with poorly performing dowels behaves similarly to one with a free edge, resulting in significantly increased stress and deflection that may compromise operational stability.

The first calculations of compressive stresses induced by dowel bars were performed by Bradbury, who assumed that each dowel bar behaved as an infinite beam resting on a Winkler foundation. Based on his analysis, he derived formulas for the dowel bar length required to resist allowable shear, bending, and bearing stresses [1]. However, the effects of dowel diameter and spacing were not analyzed in detail and were mainly inferred from empirical observations and practical assumptions of that time. Although these results had fundamental significance, they did not fully reflect the spatial behavior of the slab-joint-foundation system under load.

Subsequently, the two-dimensional finite element method (FEM) was used to analyze the response of rigid pavements [2, 3]. However, 2D models have inherent limitations because they assume plane strain or plane stress conditions, which do not allow accurate evaluation of the three-dimensional interaction between dowel bars, surface layers, and the foundation. In recent years, the rapid development of computing technology and the advantages of three-dimensional FEM have enabled more detailed analyses of rigid pavement responses, making this method increasingly popular in pavement studies [4, 5, 6, 7, 8]. Most of these studies, however, have focused on highway pavements with relatively thin slabs or on evaluating pavement performance to propose design optimizations.

Various standards and guidelines worldwide specify dowel bar dimensions and spacing based on slab thickness and load level, emphasizing the importance of dowel placement to ensure load transfer efficiency and prevent slab cracking. Some standards also include adjustment factors based on aircraft type, climatic conditions, foundation strength, and joint length. However, most of these parameters have been developed primarily under European and North American airport conditions [9, 10, 11].

Several researchers from Vietnam and many other countries, including Nguyen Quoc Van, Tran Nam Hung, Hoang Khac Tuan, Qiao Meng, and Jagadeesh A., [8, 12, 13, 14, 15] have applied FEM to analyze rigid pavements. These studies mainly focused on pavement condition evaluation to propose design optimizations and improve operational performance. However, few in-depth studies have examined the combined influence of dowel diameter and spacing on stress-strain responses at slab edges; consequently, most domestic design references still rely on foreign standards and recommendations. This situation highlights the need to develop representative numerical models as well as laboratory and field experiments suited to local airport conditions, thereby improving national rigid pavement design standards and operational reliability.

Based on these considerations, the authors employed a three-dimensional finite element approach using ABAQUS to investigate the combined effects of dowel diameter and spacing on the stress-strain response at the edges of airport cement concrete slabs. This study contributes through a detailed numerical simulation model of the contact mechanism between the dowel bars and the concrete, specifically parameterized for aircraft loading conditions and the range of airfield concrete slab thicknesses common in Vietnam. Results from the model provide a quantitative database that contributes to strengthening the scientific basis for the design and improvement of airport rigid pavements in Vietnam.

2. THEORETICAL BASIS FOR STRUCTURAL CAPACITY ANALYSIS OF RIGID PAVEMENTS

Rigid pavements began to be calculated in the 1920s of the last century, when a number of researchers proposed approximate methods to determine the required thickness of concrete slabs, typically the formulas of Goldbeck [16] and Older [17]. The formulas were based on a concentrated load P applied at the corner of the slab. In deriving their formulas, Goldbeck and Older assumed that, under loading, the foundation would settle and separate from the slab, so that only the concrete slab itself responded to the load, without considering the influence of the base layer.

The main shortcomings of this approach include neglecting the reaction of the foundation and deriving the calculation formulas from beam bending theory rather than plate theory.

The method for calculating the strength of rigid pavements of airports according to ICAO, based on the approximate solution to the problem of calculating the stress in the plate on the elastic base of Winkler, was carried out by H. M. Westergaard in 1926 [18]. To solve this problem, Westergaard studied a thin plate on the elastic base of Winkler and proposed the following approximate formulas for calculating the stress for different loading positions:

a. Loading at the corner of the slab (c)

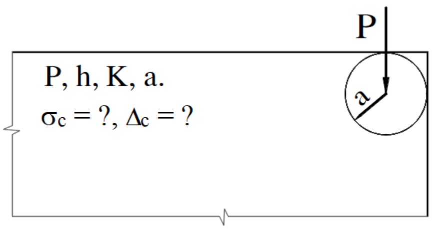

Figure 1. Loading at the corner of the slab.

Westergaard applied a successive approximation method and obtained the formula Eq. (1) for calculating stress and deflection [18]:

$$\sigma_c = \frac{3P}{h^2}\left[1-\left(\frac{a\sqrt{2}}{\ell}\right)^{0.6}\right], \qquad \Delta_c = \frac{P}{k\ell^2}\left[1.1-0.88\left(\frac{a\sqrt{2}}{\ell}\right)\right], \tag{1}$$

where: ℓ is the radius of relative stiffness; h is the thickness of the concrete slab; a is the circular radius with an area equivalent to the contact area of the wheel load; k is the foundation coefficient.

In 1985, Ioannides et al. applied the finite element method to evaluate Westergaard solutions, they proposed to use the following relationships [19]:

$$\sigma_c = \frac{3P}{h^2}\left[1-\left(\frac{c}{\ell}\right)^{0.72}\right], \quad \Delta_c = \frac{P}{k\ell^2}\left[1.205-0.69\left(\frac{c}{\ell}\right)\right]. \tag{2}$$

b. Loading at the center of the slab (i)

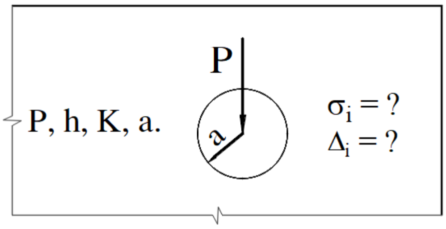

Figure 2. Loading at the center of the slab

The formula developed by Westergaard for the internal stress in a plate under a circular loading zone of radius is a as follows [18]:

$$\sigma_i = \frac{3(1+\mu)P}{2\pi h^2}\left(\ln\frac{\ell}{b}+0.6159\right), \tag{3}$$

$$b = \begin{cases} \sqrt{1.6a^2+h^2}-0.675h, \text{ if } a<1.724h; \\ a, \text{ in all other cases.} \end{cases} \tag{4}$$

For the Poisson ratio of 0.15 and in terms of base-10 logarithms, Eq. (3) can be written as:

$$\sigma_i = \frac{0.316P}{h^2}\left(4\lg\frac{\ell}{b}+1.069\right). \tag{5}$$

The deflection equation is: $\Delta_i = \frac{P}{8k\ell^2}\left\{1+\frac{1}{2\pi}\left[\ln\left(\frac{a}{2\ell}\right)-0.673\right]\left(\frac{a}{\ell}\right)^2\right\}.$

c. Loading at the edge of the slab (e)

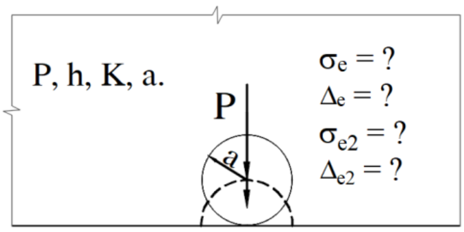

Figure 3. Loading at the edge of the slab

The stresses induced by edge loads were presented by Westergaard in several publications in 1926, 1933, and 1948 [18, 20, 21]. In his 1948 article, he provided general solutions for the maximum stress and deflection caused by circular and semi-circular loading areas applied at the slab edge. These solutions were later extended and reformulated by Ioannides et al. [19] as follows:

$$\sigma_{\underset{(circle)}{e}} = \frac{3(1+\mu)P}{\pi(3+\mu)h^2}\left[\ln\left(\frac{Eh^3}{100ka^4}\right)+1.84-\frac{4\mu}{3}+\frac{1-\mu}{2}+\frac{1.18(1+2\mu)a}{\ell}\right], \quad (6)$$

$$\Delta_{\underset{(circle)}{e}} = \frac{P\sqrt{2+1.2\mu}}{\sqrt{Ekh^3}}\left[1-\frac{(0.76+0.4\mu)a}{\ell}\right], \quad (7)$$

$$\sigma_{\underset{(semicircle)}{e2}} = \frac{3(1+\mu)P}{\pi(3+\mu)h^2}\left[\ln\left(\frac{Eh^3}{100ka^4}\right)+3.84-\frac{4\mu}{3}+\frac{(1+2\mu)a}{2\ell}\right],$$

$$\Delta_{\underset{(semicircle)}{e2}} = \frac{P\sqrt{2+1.2\mu}}{\sqrt{Ekh^3}}\left[1-\frac{(0.323+0.17\mu)a}{\ell}\right].$$

Currently, design standards in several countries, including Vietnam and Russia, calculate the edge moment of concrete slabs by applying a conversion factor to the moment at the slab center. Depending on whether the slab edge is free or connected, the corresponding factor is 1.5 or 1.2, respectively [22, 23].

3. RESEARCH ON THE EFFECT OF DISTANCE AND DIAMETER OF DOWEL BARS ON STRESS AND DEFLECTION OF AIRFIELD CONCRETE SLABS

3.1. Characteristics of pavement structure layers, aircraft loads and research model

This study developed the simulation model based on the taxiway structure S of Tan Son Nhat International Airport [24]. The characteristics of the structure are shown in Table 1.

Table 1. Concrete, base, and dowel bar properties used for the finite element model [24].

Layer	Cases	Thickness (m)	Modulus of elasticity (MPa)	Poisson's ratio
1	Concrete M350	0.40	31000	0.15
2	Concrete M150	0.38	16000	0.20
3	Crushed stone aggregate	0.18	450	0.35
4	Sand	0.50	180	0.35
5	Subgrade	2.50	130	0.40

The dowel CT3 has a length of $L = 0.60m$, elastic modulus $E = 210000MPa$ and Poisson's ratio $\mu = 0.3$.

The contact stress at the wheel-road interface is taken as the tire pressure and is evenly distributed in the contact area. The contact area used in this study is taken according to the Portland Cement Association method [25]. According to this method, the tire-road contact area is a rectangle with a length of 0.8712L and a width of 0.6L, L is calculated according to the formula:

$$L = \sqrt{\frac{P_d}{0.5227q}} \tag{8}$$

where: P_d is the load on one tire;

q is the tire pressure.

The payload of B737-500 aircraft was used in the simulation. The main characteristics of the aircraft are shown in Table 2 [10, 26].

Table 2. Characteristics of the airplanes (FAARFIELD 2.1.1)

Aircraft	Tire pressure (MPa)	Footprint area (mm^2)	Tire contact length (mm)	Tire contact width (mm)	Dual spacing (mm)	Tandem spacing (mm)
B737-500	1.338	105836	464	290	774.7	0

Consider the case where the aircraft wheel load being placed centrally next to the plate, lying entirely on the slab edge.

For this research, a model with the following parameters was developed: It consists of two 5.0 x 5.0 m concrete slabs connected by dowel bars. The dimensions of the other structural layers are shown in Figure 4.

This study is limited to the linear elastic response of the structure under operational loading. Accordingly, the materials are represented as isotropic, elastic. The contact between the material layers is modeled by tangential and normal contact behavior to the contact surface. This model does not consider time-dependent effects or damage mechanisms, including cracking, creep, or material degradation.

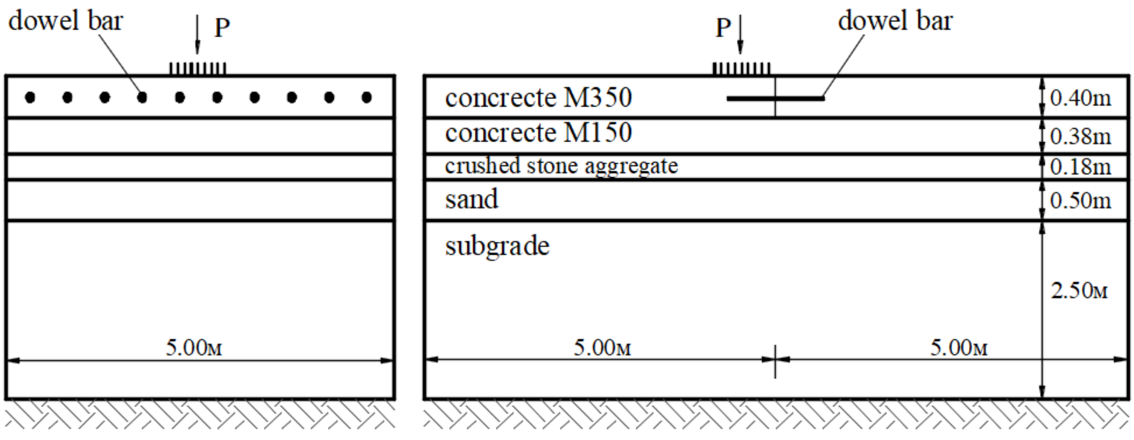

Figure 4. Research concrete pavement structure.

In the AASHTO 1993 pavement design manual, the coefficient of friction between the concrete slab and the base layer is determined through the characteristics of each type of base material. Accordingly, the coefficient of friction between the concrete slab and the base surface ranges from 0.9 to 2.2 [27]. At the location where there is an insulating layer between the two layers of material, the coefficient of friction is significantly reduced, so it is chosen to be 0.5. For the remaining layers, depending on the properties of the material, the coefficient of friction is chosen to be 1.5. The interface between half of the dowel bar in a slab and concrete modeled as a perfect bond and the other half in the neighboring slab could move along the dowel bar's axial direction. The tangential behavior of the dowel modeled using Coulomb frictional contact between the surfaces. Separation was allowed between the surfaces. The tangential behaviour of surface between the slab and base was modelled as Isotropic Coulomb friction. Loss of contact between slab and base modeled using normal hard contact that allows the surfaces to separate after coming in contact. No separation was permitted between foundation layers. The sides between the two neighboring slabs at the joint were considered to have a zero gap with a Coulomb friction of 1.5 [28, 29].

All translational degrees of freedom were restricted at the lower surface of the subgrade layer. The sides of subgrade boundaries were constrained in their Y-direction and were applied to the sides of the base as well as all side surfaces of the subbase. As portions of the concrete slab may lose contact with the base. Therefore, No exterior restrictions are used at the slabs whose stability is preserved by its interaction with the base and the slab own weight. The dowel bars were connected to the slab by the interaction properties and stabilized by their weight.

To ensure the continuity of the joint between two consecutive layers, the model uses only one type of element (C3D8R). The areas with important stresses (around the dowel bars, the contact area between the concrete slabs) are meshed more finely. Depending on the convergence of the calculation results, the calculation time, as well as depending on the problem, in this study, the number of model elements ranges from 90629 to 202101.

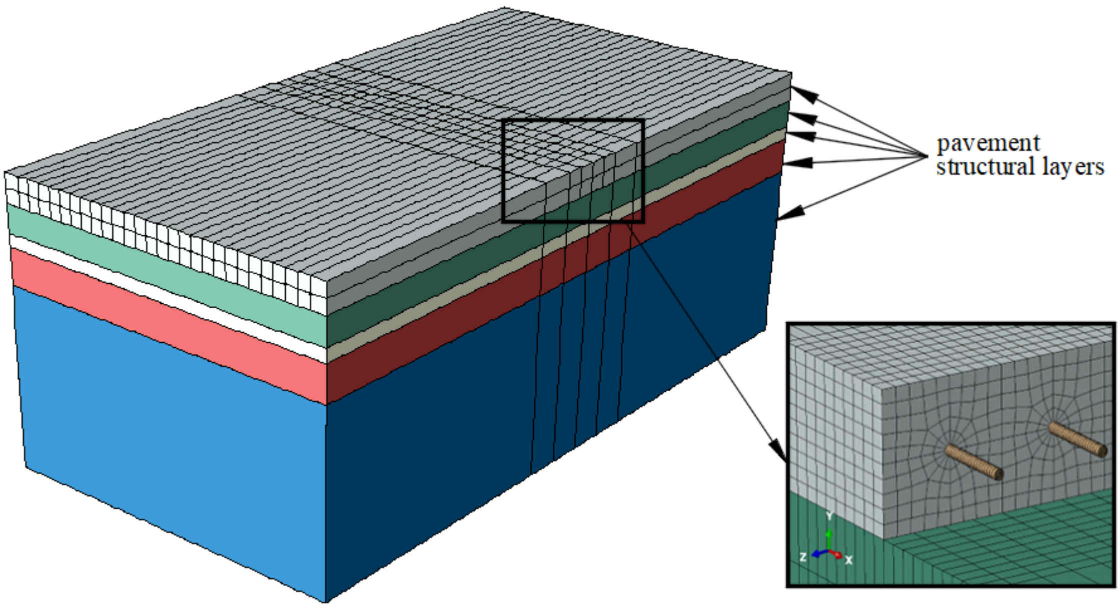

Figure 5. Finite element model in Abaqus.

This model has been proven to be highly reliable through comparison with experimental results and has been used by the author to publish some previous studies [4, 30]. In addition, some authors in the world have also used similar models for studies on rigid pavements subjected to static loads [6, 28].

3.2. Effect of spacing between dowel bars

The spacing between dowel bars is an important factor affecting the performance of concrete pavement structures, especially in controlling stress and deflection at the junction between two concrete slabs. When the spacing between dowel bars is too large, the dowel bars capacity is reduced, leading to increased local stress at the edge of the concrete slab. This can cause cracking or reduce the life of the structure due to uneven load distribution. Conversely, if the spacing between dowel bars is too small, it not only increases construction costs but also reduces overall efficiency, due to the risk of force concentration in the areas around the dowel bars.

To study this problem, a model was built using 32 mm-diameter, 0.6 m-long dowel bars to connect 2 concrete slabs, the spacing between the dowel bars was changed from 0.1 m to 1.0m. With two cases: concrete slab thickness 0.3m and 0.4m (corresponding to the common thickness range at current Vietnamese airports).

Figures 6 and 7 show the dependence of deflection and stress on the spacing between the dowel bars (along the edge of the slab with dowel bars) for a concrete slab with a thickness h = 0.4 m.

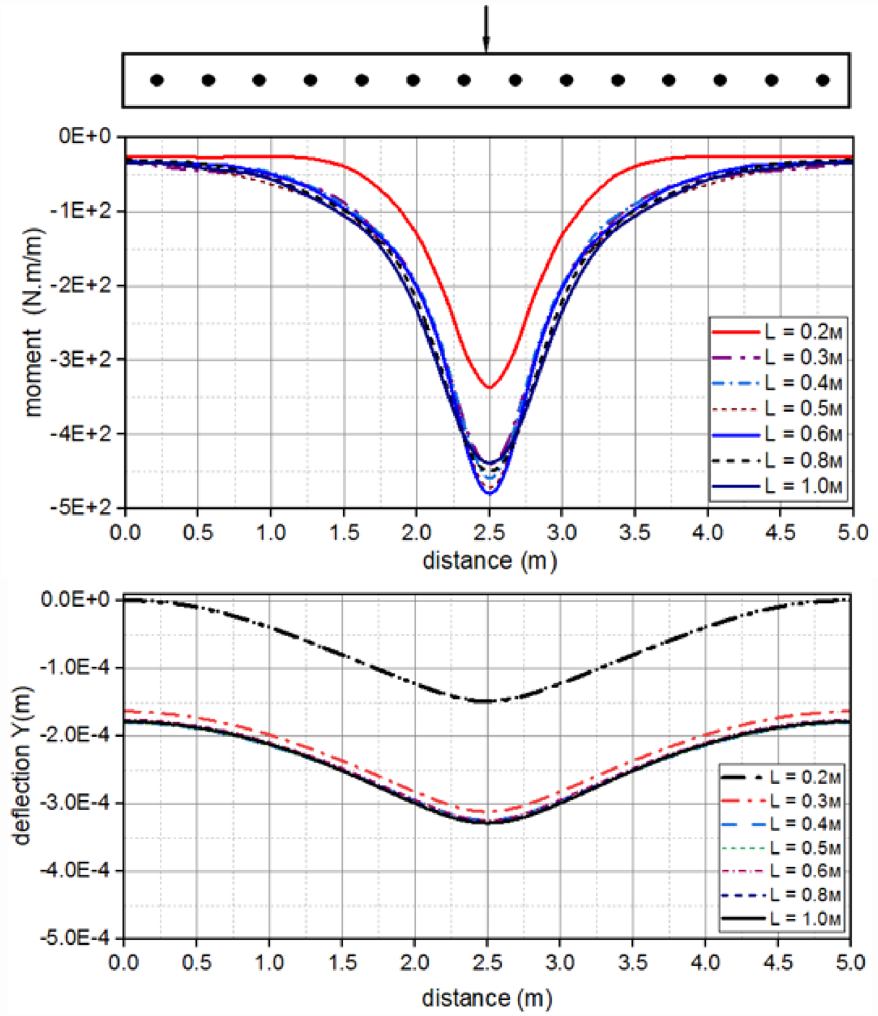

Figure 6. Moment and deflection at the bottom edge of the concrete slab according to the spacing between the dowel bars L.

The dependence of the deflection and the maximum bending moment on the spacing between the dowel bars and the thickness of the concrete slab is shown in Fig. 6. From there, we can see that when the spacing between the dowel bars increases from 0.20 m to 0.30 m, the moment and deflection increase rapidly (about 32%), when the distance is 0.40 m or more, the change is insignificant (about 8%).

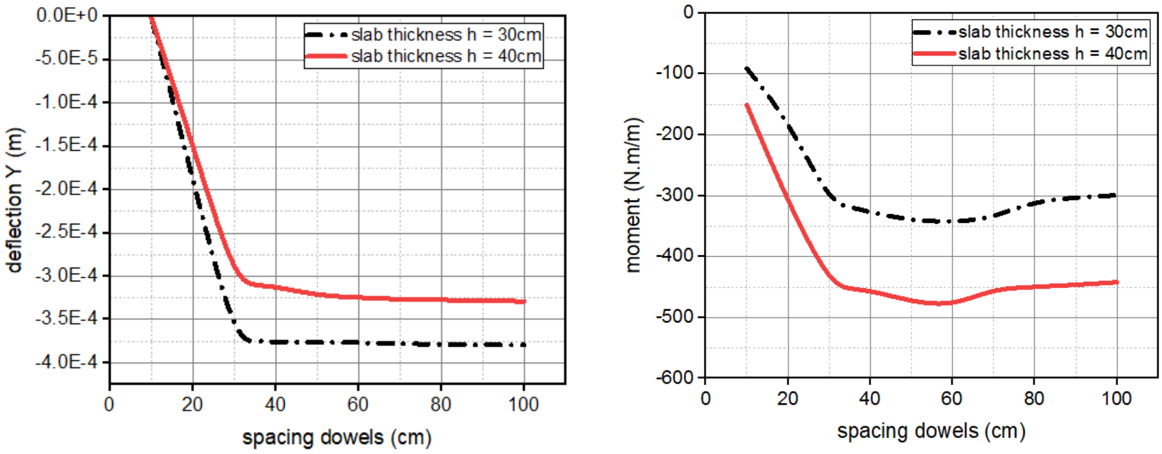

Figure 7. Dependence of deflection on spacing between dowel bars.

Data in Fig. 7 show that when increasing the thickness of the concrete slab from 0.30m to 0.40 m, the deflection will decrease and the bending moment will increase. At the same time, when the spacing between dowel bars is from 0.40 m or more, the moment and deflection are relatively stable.

Visualize the results of deflection and bending moment at the bottom edge of the concrete slab, depending on the spacing between dowel bars and the slab thickness in the form of a 3D graph (Fig. 8).

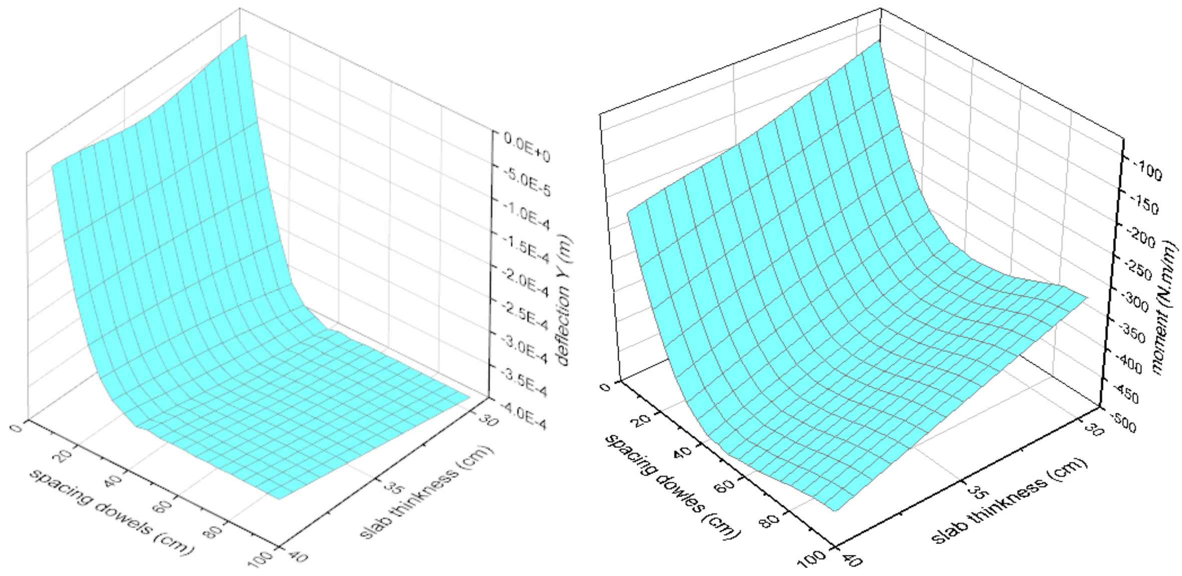

Figure 8. Relationship between deflection, moment along the thickness of the concrete slab and the spacing between the dowel bars.

The simulation results show that whether the concrete slab has a thickness of h = 0.30 m or h = 0.40 m, when the distance between the dowel bars increases to 0.40 m, the deflection and stress at the bottom of the slab increase rapidly, when the distance is 0.40 m or more, the deflection and stress are relatively stable.

3.3. Effect of the diameter of the dowel bars

The diameter of the dowel bars is an important factor affecting the load-bearing capacity and load distribution between concrete slabs in a pavement structure. Large diameter dowel bars generally increase the effective load-transfer capacity, helping to reduce tensile stress at the edge of the slab and limit deflection at the joints, which is critical for preventing cracking or deterioration under heavy loads. However, excessively large diameters can also lead to stress concentration around the bars, increasing the risk of local failure if not properly designed. By contrast, smaller diameter dowel bars will increase the steel density but may not ensure sufficient load-bearing capacity.

To study this problem, the model uses 14 dowel bars with dowel diameters varying from 20mm to 60mm, 0.6m-long.

Figure 9 shows the dependence of deflection and moment on the diameter of the dowel bars (along the edge of the slab there are dowel bars) for a concrete slab with a thickness of h = 0.40m.

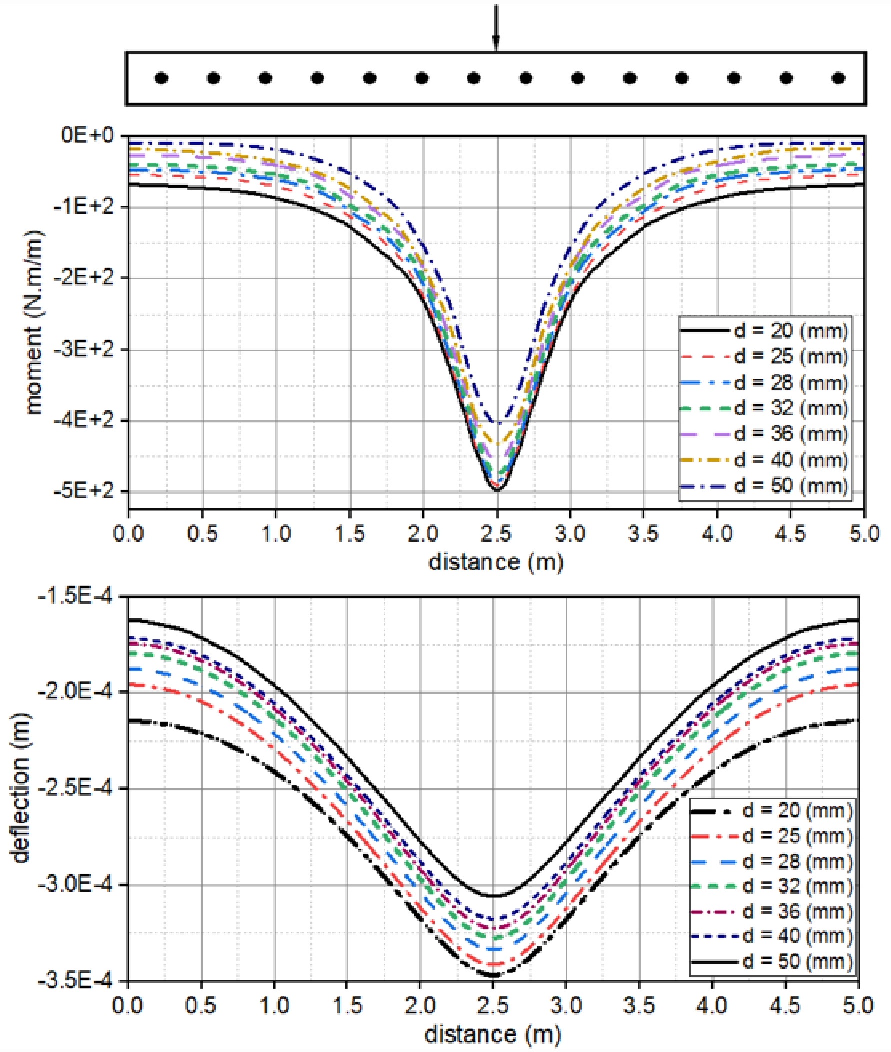

Figure 9. Deflection and moment at the edge of the slab depending on the diameter of the dowel bars.

The variation of deflection and moment at the slab edge according to the dowel bars diameter is shown in Fig. 10 (for concrete slabs with thicknesses of 0.30 m and 0.40 m).

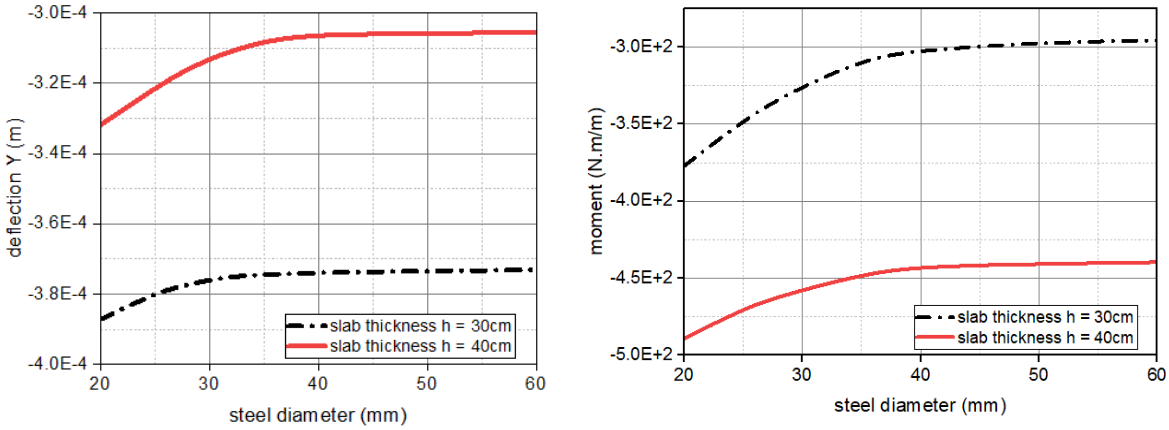

Figure 10. Variation of deflection and moment at the edge of the slab according to the diameter of the dowel bars.

Data in Fig. 9 and Fig. 10 show that the deflection is inversely proportional to the diameter of the dowel bars and the thickness of the slab. The moment is inversely proportional to the diameter of the dowel bars but directly proportional to the thickness of the concrete slab.

Visualize the results of deflection and moment at the bottom edge of the concrete slab, depending on the diameter of the dowel bars and the thickness of the slab in the form of a 3D diagram (Fig. 11).

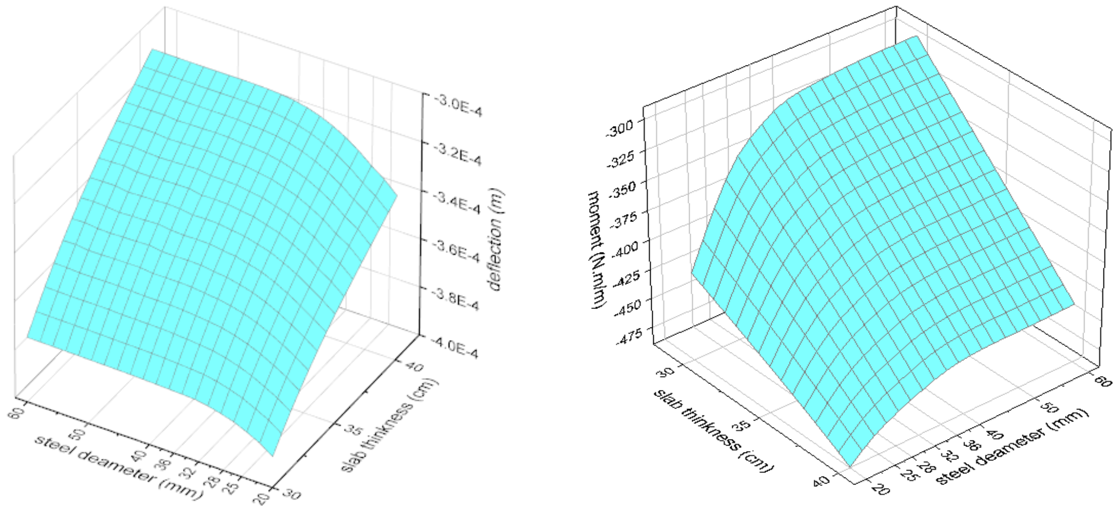

Figure 11. Deflection and moment at the edge of the slab according to the thickness of the slab and the diameter of the dowel bars.

The simulation results show that when the diameter of the dowel bars increases to 40mm, both the deflection and moment decrease rapidly, and when the diameter is 40 mm or more, the deflection and moment are relatively stable. This result is true for both 0.30 m and 0.40 m thick concrete slabs.

Table 3 presents the results of slab-edge deflection and moment from both analytical and finite element simulations for slabs 0.30 m and 0.40 m thick, with 0.6 m long dowel bars spaced 0.35 m apart.

Table 3. Comparison of results calculated by analytical and simulation methods.

Thickness slab (cm)	Diameter of dowel bar (mm)	Deflection (mm)		Error (%)	Moment (N.m/m)		Error (%)
		(1)	(2)		(1)	(2)	
h = 40	32	0.292	0.325	11.3	520.7	455	12.6
	40	0.292	0.318	8.9	520.7	445	14.5
h = 30	32	0.331	0.376	13.6	362.2	321	11.4
	40	0.331	0.374	13.0	362.2	302	16.6

Notes: (1) - calculated using the method of Westergaard and Ioannides, Eq. (6) and Eq. (7);
(2) - calculated using the finite element method.

Table 3 shows that the deflection calculated by the Westergaard and Ioannides method is smaller than that from the finite element simulation, while the edge moment of the slab is larger. It indicates that the Westergaard and Ioannides method tends to underestimate deflection, suggesting a safer evaluation of the structure in terms of serviceability, but is more conservative regarding internal forces, as it predicts larger edge moments. Such a finding may cause the designer to choose a thicker structure or arrange larger dowel bars, leading to a design that is biased towards safety but potentially has the risk of economic redundancy. The finite element method provides more realistic results on the distribution of the plate's behavior, clearly reflecting the overall performance of the plate - foundation - dowel bars. However, the results may be sensitive to modeling assumptions, requiring the designer to have experience and accurate input data (base elastic modulus, boundary conditions, friction, etc.).

In addition, the results also show that the deflection and moment of the concrete slab when using the Westergaard and Ioannides method do not depend on the diameter or spacing between the dowel bars. This reflects the oversimplification of the traditional method, which assumes the slab to work in a single state on an elastic foundation and does not consider the force interaction between neighboring slabs. Meanwhile, the finite element method allows detailed simulation of the influence of the dowel bars, thereby more accurately assessing the load transfer efficiency, especially at airports operating heavy aircraft.

4. DISCUSSION

Calculations of the three-dimensional finite element model were performed for concrete slab under static load of B737-500 aircraft with different cases of spacing (0.1, 0.2, 0.3, 0.4, 0.5, 0.6, 0.8, 1.0m), diameter (20, 25, 28, 32, 36, 40, 50, 60mm), 0.6m length of the dowel bars and thickness of the concrete slab (0.30, 0.40m). Other parameters, such as modulus, connection of the concrete slab to the sub-layers, loads, and boundary conditions, remained unchanged.

Figures 6 and 7 show that, for a constant dowel bar diameter, both deflection and stress increase rapidly as the spacing between dowel bars grows from 0.10 m to 0.40 m (deflection increases by 2.2 times and stress by 1.4 times). Beyond 0.40 m, deflection and stress remain almost unchanged.

Figures 9 and 10 show that, when the diameter of the dowel bars increases from 20 mm to 40 mm, deflection and stress decrease by 1.1 times, while further increases beyond 40 mm result in minimal changes. The 3D diagrams in Fig. 8 and Fig. 11 illustrate this variation more intuitively.

When calculated using Westergaard's and Ioannides's method, the deflection will be smaller than the finite element simulation method (from 8.9% to 13.6%), and the moment at the edge of the plate will be larger (from 11.4% to 16.6%). This deviation has many reasons, such as: boundary conditions, interaction between the plate and the foundation, and assumptions when calculating.

Table 4 compares the calculation results from this study with the regulations on diameter and spacing between the dowel bars in current standards of Vietnam and some countries in the world.

Table 4. Dimensions and spacing of dowel bars.

Method	Thickness of slab (cm)	Diameter (mm)	Spacing (cm)
According to research	30-40	30-40	30-40
TCVN 10907-2015 [22]	31-45	30-40	30
Russia [23]	31-40	32	30
China [31]	30-40	30-32	35
FAA (America) [10]	32-41 (12.5-16.0 in)	30	38

The results in Table 4 have strongly confirmed the findings of this study. The determined reasonable parameter range (diameter: 30-40 mm, spacing: 0.30-0.40 m) shows a strong agreement with the main international standards (Russia, China, USA) and the Vietnamese standard. More importantly, the study has identified a selection range, providing engineers with more flexibility in choosing the diameter and spacing between the dowel bars while ensuring structural performance.

On that basis, it is recommended to configure the design and arrangement of the dowel bars with the current parameters. Future studies will expand on this investigation by exploring a broader range of influencing factors, including thermal and dynamic loads of different aircraft types, as well as taking into account the nonlinear properties of concrete.

5. CONCLUSION

Reasonable spacing and diameter when arranging dowel bars helps to distribute force evenly, reduce tensile stress at the edge of the slab and limit adverse deflection. In addition, it also ensures synchronous operation between concrete slabs under the impact of aircraft loads. Research on this influence plays an important role in the design of concrete pavements, to ensure sustainability and economic efficiency in the construction of airport works.

Using the three-dimensional finite element method, the authors studied the influence of diameter and spacing between dowel bars on stress and deflection of airport pavement concrete slabs. The research results show that:

- This method can take into account the influence of many factors affecting deflection and stress in the concrete slab that the analytical method has not taken into account.

- Deflection is inversely proportional to the thickness of the concrete slab, while stress is directly proportional to the thickness. At the same time, when the spacing between the dowel bars exceeds 0.40 m, the deflection and stress do not change much.

- When arranged at the same distance, if the diameter of the dowel bars increases, it will lead to a decrease in deflection and stress. However, when the dowel bar diameter exceeds 40 mm, both deflection and stress remain largely unchanged.

Based on the results presented, it is recommended that airport cement concrete pavements employ dowel bars with diameters of 30 - 40 mm, spaced 0.30 - 0.40 m apart, for concrete slabs 0.30-0.40 m thick.

REFERENCES

[1]. R. D. Bradbury, Design of joints in concrete pavements, In Proceedings of the 12th annual meeting of the Highway Research Board, Washington D.C., 1932, pp. 105-141.

[2]. Y. H. Huang, A computer package for structural analysis of concrete pavements, In Proceedings of the 3rd International Conference on Concrete Pavement Design and Rehabilitation, Purdue University, West Lafayette, 1985, pp. 295-307.

[3]. A. M. Tabatabai, E. J. Barenberg, Finite-element analysis of jointed or cracked concrete pavements, Transportation Research Board, Washington D.C., 1978, pp. 11-19.

[4]. V. V. Tatarinov, Tien Dung Vo, Calculation of the edge zone of the airfield pavement slab using the finite element method, Design construction and operation of airfields: collection of scientific papers, Tekhnopoligraftsentr, 2025, pp. 6-16 (in Russian).

[5]. Tien Dung Vo, Van Hieu Nguyen, Van Thuy Do, Huu Lam Nguyen, Research on application of finite element method to analyze load transfer efficiency according to deflection of airport rigid pavement, Journal of Science and Technique, 07 (2024) 7-18. https://doi.org/10.56651/lqdtu.jst.v7.n01.825.sce

[6]. Piotr Mackiewicz, Finite-Element Analysis of Stress Concentration around Dowel Bars in Jointed Plain Concrete Pavement, Journal of Transportation Engineering, (2015) 06015001-1-8. https://dx.doi.org/10.1061/(ASCE)TE.1943-5436.0000768

[7]. Antoni Szydlo, Piotr Mackiewicz, Thermal Stress Analysis in Concrete Pavements, Journal of Transportation Engineering, Part B: Pavements, 73 (2020) 06020002-1-11.

[8]. Hoang Khac Tuan, Pham Ngoc Thach, Cement concrete pavement on elastic foundation: Behavior due to temperature difference and simultaneous vehicle load, Proceedings of the school-level scientific conference, 2022, pp. 139-149 (in Vietnamese).

[9]. UFC 3-260-02, Pavement Design for Airfields, Washington, DC: Department of Defense, 2001.

[10]. AC 150/5320-6G, Airport Pavement Design and Evaluation, Washington, DC: U.S. Department of Transportation, 2021.

[11]. AC 150/5320-6F, Airport Pavement Design and Evaluation, Washington, DC: U.S. Department of Transportation, 2016.

[12]. Nguyen Quoc Van, Trinh Trung Tien, Research on thermal stress in cement concrete slabs, Vietnam Bridge and Road Journal, 2022, pp. 48-51 (in Vietnamese).

[13]. Tran Nam Hung, Le Van Phuong, Analysis of heat transfer in cement concrete pavement using three-dimensional heat transfer model, Journal of Science and Technology, 2019, pp. 112-121 (in Vietnamese).

[14]. Qiao Meng, KeZhong and Mingzhi Sun, Dynamic Response Analysis of Airport Pavement under Impact Loading, Appl. Sci., 13 (2023) 5723. https://doi.org/10.3390/app13095723

[15]. A. Jagadeesh, W. A.A.S. Premarathna, A. Kumar, C. Kasbergen, S. Erkens, Finite element modelling of jointed plain concrete pavements under rolling forklift tire, Engineering Structures, 328 (2025) 119705. https://doi.org/10.1016/j.engstruct.2025.119705

[16]. A. T. Goldbeck, Thickness of Concrete Slabs, Public Roads,1 (1919) 34-38.

[17]. C. Older, Highway Research in Minors, Transactions of the American Society of Civil Engineers. vol.87, 1924.
[18]. H.M. Westergaard, Stresses in Concrete Pavements Computed by Theoretical Analysis, Public Roads 7 (1926) 25-35.
[19]. A. M. Ioannides, M. R. Thompson M and E. J. Barenberg, Westergaard Solutions Reconsidered, Transportation Research Record 1043, Transportation Research Board, 1985, pp. 13-23.
[20]. H. M. Westergaard, New Formulas for Stresses in Concrete Pavements of Airfields, Transactions American Society of Civil Engineers, 113 (1948)425-439.
[21]. H. M. Westergaard, Analytical Tools for Judging Results of Structural Tests of Concrete Pavements, Public Roads, 14 (1933) 185-188.
[22]. TCVN 10907:2015, Civil Aerodrome - Pavement - Specifications for Design, Directorate for Standards, Metrology and Quality, 2015 (in Vietnamese).
[23]. SP.121.13330-2019, SNiP 32-03-96 Airfields, Ministry of Construction and Housing and Communal Services of the Russian Federation, 2019 (in Russian).
[24]. Saigon Asia Inspection and Consulting Joint Stock Company, Report on measuring and evaluating the load-bearing capacity of taxiway S, runway surface of Tan Son Nhat International Airport, 2022 (in Vietnamese).
[25]. PCA, Design of Concrete Airport Pavement, Portland Cement Association, 1955.
[26]. FAARFIELD (Version 2.1.1) [Computer software], FAARFIELD Aircraft Database, FAA Aviation Data Center, 2023. https://www.airporttech.tc.faa.gov/Products/Airport-Safety-Papers-Publications/Airport-Safety-Detail/faarfield-211
[27]. AASHTO, Guide for Design of Pavement Structures, Washington, DC: American Association of State Highway and Transportation Officials, 1993.
[28]. Ahmed Ebrahim Abu El-Maaty, Ghada Mousa Hekal and M. Eman Salah El-Din, Modeling of Dowel Jointed Rigid Airfield Pavement under Thermal Gradients án Dynamic Loads, Civil Engineering Journal, 2 (2016) 38-51.
[29]. S. R. Maitra, K. S. Reddy, L. S. Ramachandra, Estimation of Critical Stress in Jointed Concrete Pavement, Procedia Social and Behavioral Sciences, 104 (2013) 208-217.
[30]. Van Thuy Do, Van Hieu Nguyen, Tien Dung Vo, Huu Lam Nguyen, Analysis of theoretical basis for assessing the bearing capacity of airport cement concrete pavement in Vietnam by the dynamic deflection equipment, Journal of Science and Technique, 61 (2023) 63-75. https://doi.org/10.56651/lqdtu.jst.v6.n01.667.sce
[31]. MH/T 5004-2025, Specifications for Airport Cement Concrete Pavement Design, Civil Aviation Administration of China - CAAC, 2025 (in Chinese).